JOURNAL OF Materials CHEMISTRY

Porphyrins entrapped in an alumina matrix

Omar J. de Lima,[a] Daniel P. de Aguirre,[a] Daniela C. de Oliveira,[a] Moisés A. da Silva,[a] Cesar Mello,[b] Carlos A. P. Leite,[b] Hérica C. Sacco*[a] and Katia J. Ciuffi*[a]

[a] *Universidade de Franca, Av. Dr. Armando Salles Oliveira, 201, 14404-600 Franca, SP, Brazil. E-mail: katiapedro@netsite.com.br; hcsacco@netscape.net; Fax: (+55 16) 3711 8886*
[b] *Instituto de Química, UNICAMP, Campinas-SP, Brazil*

Received 25th January 2001, Accepted 14th June 2001
First published as an Advance Article on the web 9th August 2001

Novel hybrid organic–inorganic catalysts constituted by iron(III) or manganese(III) 5,10,15,20-tetrakis(pentafluorophenyl) porphyrin entrapped in an alumina amorphous matrix have been prepared. The hybrid materials were obtained by a non-hydrolytic sol–gel route, through the condensation of aluminium chloride with diisopropyl ether in the presence of metalloporphyrin. The presence of the metalloporphyrin entrapped in the alumina matrix is confirmed by ultraviolet–visible spectroscopy and electron spectroscopic imaging. The material was also analysed by infrared spectroscopy, selected area diffraction, scanning electron microscopy, thermogravimetric analysis and differential thermal analysis, and its surface area was determined. Comparison between the leaching of metalloporphyrin from non-hydrolytic materials and adsorbed metalloporphyrin on commercial neutral alumina confirms that in the non-hydrolytic materials the metalloporphyrin is entrapped and not just adsorbed on the alumina surface. The use of a conventional hydrolytic sol–gel process leads to the complete leaching of the metalloporphyrin from the matrix, underlining the importance of the non-hydrolytic alumina gel process in the matrix preparation. The prepared alumina matrix materials are amorphous, even after heat treatment up 270 °C.

The new catalysts prepared were tested for their ability to catalyse the epoxidation of (*Z*)-cyclooctene using iodosylbenzene as oxygen donor, giving high yields in the epoxidation, similar to those obtained using the metalloporphyrin in solution or supported on a silica matrix.

1 Introduction

Mimicking the ability of cytochrome P-450 to oxidise organic substrates by synthetic metalloporphyrins (MeP) as catalysts is well documented in the literature.[1–3] Supporting a metalloporphyrin on an insoluble resin or matrix has been the goal of several researches in the past few years.[4] The objective is to prepare a catalyst that is easy to separate, intact, from the reaction medium, with improved stability of the MeP under the reaction conditions, preventing dimerization or aggregation, and to tune the selectivity of the reaction.[5] Commonly, MeP immobilizations use covalent binding or non-covalent binding such as surface adsorption and entrapment.[2,4] Recent work[6,7] reports the synthesis and application in heterogeneous catalysis of a new class of hybrid organic–inorganic materials containing MeP entrapped on a silica matrix, prepared by a sol–gel process. These new hybrid organic–inorganic materials can catalyse oxidation reactions.

Even though there is a large number of reports using silica as a solid matrix for MeP, aluminium oxide (alumina) can also be used. Aluminas are porous solids and find applications mainly as adsorbents, catalysts and catalyst supports.[8] Sol–gel processing of alumina has created novel applications and has improved some of its properties.[9] Products such as catalyst supports, abrasives, optical fibers, films for electronic applications, aerogels, and membranes for molecular filtration have been developed on a laboratory scale based on sol–gel processing.[9] The use of the sol–gel process for the entrapment of MeP in an alumina network could lead to the preparation of new materials, with both specific surface area and controlled microstructural properties.

This work describes the optimised conditions for the preparation of new catalyst systems where iron(III) or manganese(III) 5,10,15,20-tetrakis(pentafluorophenyl) porphyrin are entrapped in a non-hydrolytic alumina matrix (MeP**NHG**) by a non-hydrolytic sol–gel process. Pentafluorophenyl porphyrins have been used instead of porphyrins due to their higher stability and activity. The MeP**NHG** materials were characterised by ultraviolet–visible (UV–Vis) spectroscopy, infrared spectroscopy (FTIR), thermogravimetric and differential thermal analysis (TGA/DTA), scanning electron microscopy (SEM), electron spectroscopy imaging (ESI), selected area diffraction (SAD) and surface area measurements. After characterisation of these new MeP**NHG** materials, we investigated their activity as catalysts for the epoxidation of (*Z*)-cyclooctene using iodosylbenzene or hydrogen peroxide as the oxygen donor. The catalytic activity of MeP**NHG** was also compared with that of MeP in homogeneous solution and MeP supported on a silica matrix, such as imidazole propyl gel (IPG)[10] and silica prepared by a sol–gel process (MePS).[7b]

2 Experimental

2.1 Materials

All solvents and reagents were of commercial grade (Merck and Aldrich) unless otherwise stated. Dichloromethane (DCM) was suspended over anhydrous $CaCl_2$ for 2.5 h, then filtered and distilled over P_2O_5 and held over 0.4 nm molecular sieve. Pyrrole was distilled under reduced pressure immediately before use. *N*,*N*-Dimethylformamide (DMF) was stirred over KOH at room temperature overnight, decanted and then distilled at reduced pressure. (*Z*)-Cyclooctene purity was determined by gas chromatographic analysis and was purified by column chromatography on basic alumina just prior to use.

5,10,15,20-Tetrakis(pentafluorophenyl) porphyrin (H_2TFPP)

DOI: 10.1039/b100897h

was prepared by the methodology of Lindsey *et al.*:[11] 2.8 g of pure H_2TFPP (43% yield) were obtained. UV–Vis (DCM) λ_{max}: 410, 508, 582, 630 nm.

Metal insertion onto H_2TFPP was performed as described by Adler, Longo and coworkers[12] by refluxing the free-base porphyrin with iron(II) chloride or manganese(II) chloride in DMF under an argon atmosphere: FeTFPPCl (90% yield), MnTFPPCl (80% yield). FeTFPPCl: UV–Vis (DCM): λ_{max} (ε/mol^{-1} L cm^{-1}): 352, 412 (1.8×10^5, Soret band) 504 (1.7×10^4), 576, 630 nm. MnTFPPCl: UV–Vis (DCM): λ_{max} (ε/mol^{-1} L cm^{-1}): 366, 460 (7.3×10^4, Soret band) 574 nm.

Preparation of metalloporphyrin entrapped in alumina (MePNHG) by a non-hydrolytic sol–gel process. The preparation of gels was carried out in oven-dried glassware. The material was synthesised *via* a modification of the method described by Acosta *et al.*[13] 1.0 mol L^{-1} of aluminium chloride ($AlCl_3$) and 1.5 mol L^{-1} of diisopropyl ether (Pr^i_2O) were reacted in the presence of 1.4×10^{-5} mol of FeTFPPCl or MnTFPPCl at reflux for 3 h at 110 °C in 50 mL of dry DCM (previously distilled) under an argon atmosphere. Aluminium chloride was solubilized by the formation of an addition complex with ether. The ether acted as the only oxygen donor.[13,14] The condenser was set up in a thermostatic bath at –5 °C. The gel was formed after 90 min of reaction, and after another 30 min a solid material began to precipitate. After reflux, the mixture was slowly cooled and aged overnight in the mother liquor at room temperature. The solvent was then slowly removed under vacuum. The obtained solid was washed with several solvents in the following order: acetone, methanol, water, methanol, acetone and DCM, and heat-treated at 60 or 270 °C. The amount of leached MeP from the MeP**NHG** materials was quantified by measuring the amount of MeP in the combined washings *via* UV–Vis spectroscopy.

Preparation of MeP entrapped on hydrous alumina. Hydrous alumina gel was prepared by reaction of 5.75 g (2.38×10^{-5} mmol) $AlCl_3{\cdot}6H_2O$ with 10 mL aqueous NH_3 (6 mol L^{-1}) in 10 mL H_2O.[15] The precipitated hydroxide was aged for 20 h and afterwards filtered and washed with pure water. It was then made into a clear sol by peptising with acetic acid under reflux at 90 °C . The sol was cooled and then mixed with 3 mg (2.91×10^{-3} mmol) of porphyrin. Gelation was performed by dehydration of the aqueous sol at room temperature. The resultant xerogel was ground and washed with several solvents in the following order: acetone, methanol, water, methanol, acetone and DCM. The amount of leached MeP from hydrous alumina was quantified by measuring the amount of MeP in the combined washings *via* UV–Vis spectroscopy.

Preparation of supported MeP on alumina. MeP supported on commercial neutral alumina was achieved by stirring a DCM solution of MeP with a suspension of alumina for 40–50 min. The resulting supported catalyst was washed with DCM and its UV–Vis spectrum was determined. The supported MeP was then washed with methanol. The loadings of MeP on alumina were quantified by measuring the amount of unloaded MeP in the combined solvent washings by UV–Vis spectroscopy.

The electronic spectra of the polymers were recorded on a UV–Vis spectrophotometer (Hewlett-Packard 8453, Diode Array). The spectra of the solid in DCM were recorded using a 2.0 mm path length cell. Better quality spectra were obtained using DCM as the solvent, where the suspension was prepared.

Thermogravimetric analysis (TGA/DTA) was carried out on a Thermal Analyst 2100 – TA Instruments SDT 2960 – Simultaneous DTA-TGA, in air with a heating rate of 10 °C min^{-1}, from 25 to 1000 °C.

Specific surface areas were determined by analysing the nitrogen adsorption isotherms according to the BET method[16] using a physical adsorption analyser (Micrometrics AccSorb 2100E).

Scanning electron microscopy (SEM) of alumina materials was performed on ground samples. The samples were coated with a conducting layer of gold by sputter coating. The images were obtained using a Digital Scanning Microscope DSM 960 Zeiss.

ESI samples were prepared by grinding the material and depositing the particles on carbon-coated palladium film supported in 300 mesh-capped grids. A Carl Zeiss CEM 902 transmission electron microscope, equipped with a casting-Henry filter spectrometer within the column, was used. Clear areas in the elemental distribution maps correspond to element-rich domains. Elemental images were observed for the relevant elements found in this sample, using monochromatic electrons corresponding to the silicon L-edge and iron M-edge with an energy-selecting slit of 20 eV in width. The energy-selecting slit was set at 1570 ± 10 eV for Al and 730 ± 10 eV for Fe (L_3 -708 eV, L_2 -721 eV). Images were recorded by a slow scan CCD camera (PROSCAM) digitised with $1024 \times 1024 \times 8$ bits. Images were processed using the ANALYSIS 3.0 software. The three-window technique was used to perform the background subtraction for each elemental image.[17]

FTIR spectra were obtained from MeP**NHG** in KBr pellets using a Perkin Elmer FTIR 1600.

Synthesis of iodosylbenzene (PhIO) was carried out through the hydrolysis of iodosylbenzene diacetate.[18a] Its purity was measured by iodometric assay.[18]

The cyclooctene oxidation reactions were carried out as control reactions in the presence of **NHG** alumina without MeP.

Into a 4 mL vial sealed with a Teflon-coated silicone septum containing 0.01 g of MeP**NHG**, 1000 µL 1,2-dichloroethane, 150 µL (*Z*)-cyclooctene and 5 µL cyclohexanone (internal standard) were added iodosylbenzene or (*ca.* 5.00 mg) hydrogen peroxide. The products were analysed by gas chromatography. These analyses were carried out using a chromatograph (HP 6890) equipped with a hydrogen flame ionisation detector and capillary column (length 30 m, inner diameter 0.25 mm). Products formed were identified by comparison of their retention times with those of authentic samples. Yields were determined by using an internal standard (cyclohexanone) and were based on the oxidant added.

At the end of the reaction, the MeP**NHG** catalyst was recovered by centrifugation and washed five times with 1 mL methanol to ensure that any remaining iodosylbenzene was removed from the catalyst. The catalyst was then dried for 3 h at 60 °C before being used again in a further oxidation reaction.

3 Results and discussion

The FeTFPPCl or MnTFPPCl was entrapped in the alumina matrix (Fig. 1) by a non-hydrolytic sol–gel route, generating non-hydrolytic gels (**NHG**), prepared by the reaction between aluminium chloride and Pr^i_2O[13,19] in the presence of MeP. The method is based on the condensation of aluminium halides with ether, through the cleavage of the O–R bond and the formation of an alkyl halide [eqn. (1)].

$$AlX_3 + 3/2ROR \rightarrow AlO_{3/2} + 3RX \qquad (1)$$

Alumina gelation originates from alkoxide–halide non-hydrolytic condensation,[13,19] with the release of alkyl halide. The alkoxide is produced *in situ* from aluminium chloride and Pr^i_2O through the formation of a Lewis adduct, followed by the nucleophilic displacement on carbon [eqn. (2)].[13,14]

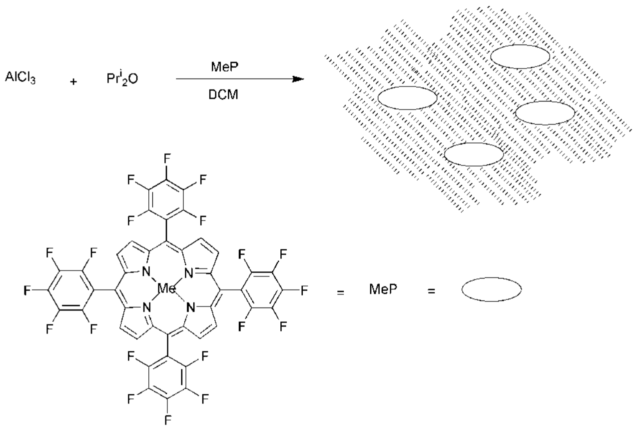

Fig. 1 Preparation of Me**PNHG**.

$$AlCl_3 + ROR \rightarrow ROAlCl_2 + RCl \tag{2}$$

Aluminium chlorides in the presence of aluminium alkoxides or chloroalkoxides are prone to giving μ-Cl- and μ-OR-bridged structures,[20] giving rise to two types of reaction: (a) nucleophilic attack of Cl at the eletrophilic aluminium atom; and (b) formation of an Al–O–Al linkage by nucleophilic attack of Cl at the electrophilic carbon atom.[13]

Maintaining reflux after gelation gives rise to precipitation of the Me**PNHG** powder. Precipitation continues through aging in the mother liquor and during the slow removal of solvent. Absence of or short aging times reduces the yield of alumina material and makes possible the leaching of MeP from the alumina matrix (*ca.* 15% of MeP is leached from the matrix). In all cases, no leaching of MeP from the Me**PNHG** was observed and we obtained 100% loading of MeP, except for Fe**PNHG** heat-treated at 60 °C where a loading of 97% FeP was observed.

The entrapment of FeP or MnP in the alumina matrix was confirmed by the presence of characteristic FeP and MnP Soret bands in the UV–Vis spectra of Fe**PNHG** and Mn**PNHG** (Table 1). The Me**PNHG**-entrapped samples have the spectrum of the corresponding metalloporphyrin in solution, indicating that the structures of FeP and MnP were preserved in the matrix. UV–Vis spectroscopy of FeP provides information on the spin and oxidation state of the iron atom from the Soret peak (typically near 400 nm) and the less intense α and β bands (between 500 and 700 nm).[21] Although the Soret peaks of Fe**PNHG** materials were resolved (Table 1) the α and β bands could not be assigned due to the presence of the solid matrix. The spectra of entrapped MnP contained the same peaks as observed for these systems in solution (Table 1).

The choice of a non-hydrolytic alumina gel process was of significant importance for obtaining the entrapped FeP, since the use of the conventional hydrolytic sol–gel process[15] leads to the complete leaching of FeP from the matrix in its dimeric form.

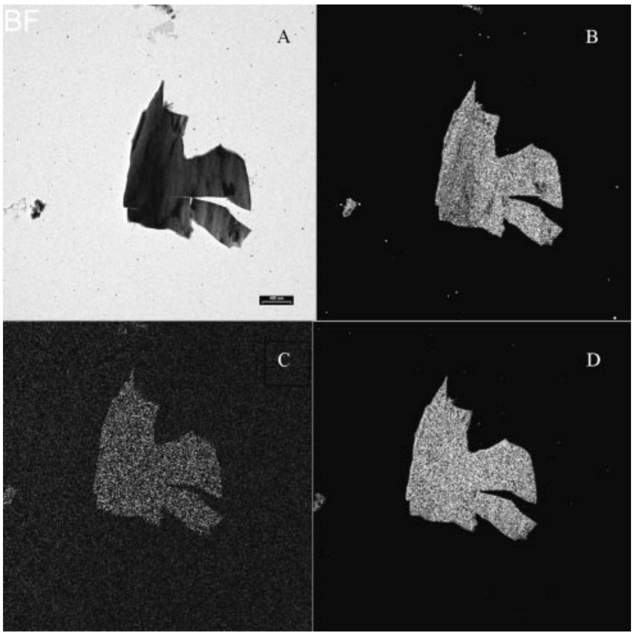

Fig. 2 ESI images of Fe**PNHG**: (A) brightfield; (B) darkfield; (C) aluminium map; (D) iron map.

To confirm that FeTFPPCl and MnTFPPCl were entrapped within the Fe**PNHG** and Mn**PNHG** materials and not just adsorbed on the surface of the alumina matrix, the same MeP samples were adsorbed on the surface of a commercial neutral alumina by stirring a suspension of commercial neutral alumina in a solution of MeP in DCM. After anchoring, the MeP was partially leached (*ca.* 60% MeP leaching) when the material was washed with DCM. Even though the starting FeP was used in its monomeric form, the adsorbed FeP material in DCM presented UV–Vis spectra characteristic of FeP in its dimeric form (Table 1). It is known that when steric factors permit, as in the case of FeTFPPCl, FeP is capable of forming oxo-bridged dimers.[21–23] In fact, chromatographic purification of FeTFPP using alumina as adsorbent leads to the formation of dimers.[23] We observed the leaching of 100% MeP in the adsorbed materials when methanol was used as solvent, and FeP was leached in its dimeric form.[23] The absence of leaching in the Me**PNHG** materials confirmed that in these materials the MeP was indeed entrapped and not simply adsorbed on the surface of alumina matrix.

The electron spectroscopic image of Fe**PNHG** shows the homogeneous distribution of the elements Fe and Al (Fig. 2). Even though the Fe image has less contrast than the Al image, they confirm that the FeP is entrapped within the alumina matrix. The electron images of Fe**PNHG** and Mn**PNHG** materials heat-treated at 60 °C were those of a non-crystalline microstructure. Indeed, Acosta *et al.*[13] showed that with this non-hydrolytic sol–gel methodology the formation of hydrated crystalline alumina gels such as bohemite (AlO(OH)) was not possible[13,19] and that the non-hydrolytic alumina so formed

Table 1 Properties of Fe**PNHG** and Mn**PNHG**: UV–Vis spectra[a] and decomposition temperatures obtained by TGA

		TGA decomposition temperature/°C		
Complex	UV–Vis spectra/nm	H_2O	Residual groups	MeP
FeTFPPCl	352, 412, 504, 576, 630	—	—	420–630
Dimeric FeTFPP	406, 566			
Fe**PNHG**	326, 414	30–202	202–420	420–630
FeP–commercial alumina	406, 566			
FeP–hydrous alumina	—[b]			
Mn^{III}TFPPCl	366, 460, 574	—	—	313–580
Mn**PNHG**	366, 458, 576	30–280	280–313	313–590

[a]UV–Vis spectra in DCM. [b]100% FeP leached from alumina, FeP bands not observed.

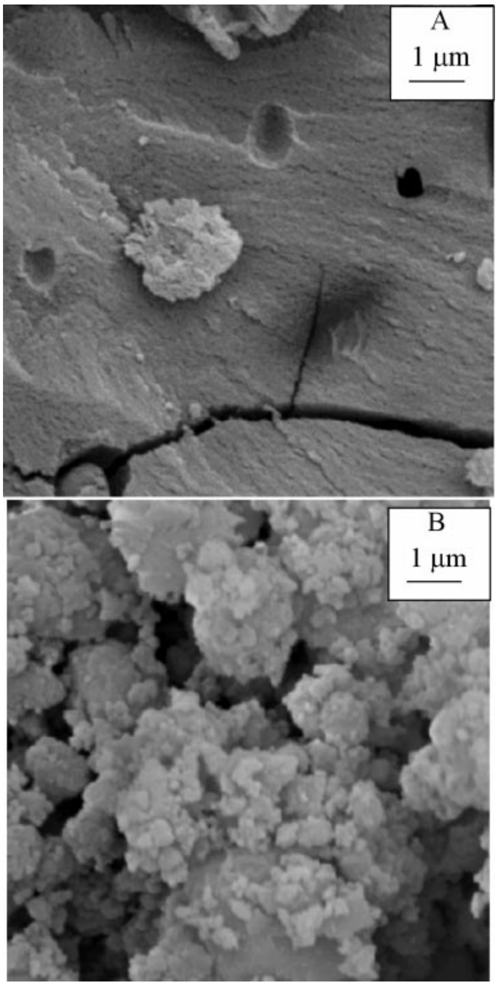

Fig. 3 SEM images of FePNHG treated at: (A) 60 °C; (B) 270 °C.

remained amorphous even after being calcined at 750 °C. The MePNHG heat treatment temperature of 750 °C led to MeP decomposition, confirmed by the disappearance of the characteristic Soret band of MeP in the UV–Vis spectra of MePNHG. The SAD technique confirmed the non-crystalline character of the samples.

The amorphous character of the **NHG** alumina precludes the IR bands characteristic of crystalline alumina in the obtained MePNHG materials,[24] and the broad bands observed cover the IR bands of MeP if MeP is present in low concentration compared with the alumina matrix. The broad band in the region 3400 cm^{-1} (hydroxyl-stretching band) indicates the presence of water adsorbed in the material, which probably occurred after its preparation.[24]

Thermogravimetric analysis of MeP**NHG** in air (Table 1) indicated that weight losses occurred mainly between 20 and 600 °C, varying from 20 to 60%. The initial weight losses on MeP**NHG** materials from 20 to 250 °C correspond to the loss of water molecules weakly bound in the MeP**NHG** materials. We observed weight losses corresponding to the pyrolysis and the oxidation of residual alkyl halide groups[13] (RX groups in eqn. (1)) between 250 and 400 °C, whereas MeP decomposition occurred between 400 and 630 °C. MeP decomposition between 400 and 630 °C in the MeP**NHG** materials is in agreement with pure MeP decomposition observed between 313 and 630 °C.[7] DTA showed one exothermic transformation at 876 °C, in a region where no weight loss was observed by TGA. This is in agreement with the results presented by Acosta *et al.*[13] and is ascribed to the appearance of a more ordered transition phase of alumina (γ-alumina).

SEM images of FeP**NHG** materials heat-treated at 60 and 270 °C are similar to those of the corresponding MnP**NHG** and are shown in Fig. 3. When we compare the morphologies of MeP**NHG** materials heat-treated at 60 and 270 °C we observe very different surface properties in both materials. The former material is compact and has a smooth surface, whereas the FeP**NHG** heat-treated at 270 °C is rough and particulate and is constituted of loose particles. The difference in the morphologies could be attributed to the difference in the heat treatment processes. The heat treatment at 270 °C removes the solvent molecules present in the solid matrix, producing a surface rougher and more particulate than that of the FeP**NHG** heat-treated at 60 °C. The surface area of these materials confirms that. Both FeP**NHG** and MnP**NHG** materials heat-treated at 60 °C present a low specific surface area ($< 5\ \mathrm{m}^2\ \mathrm{g}^{-1}$) indicating that they have formed compact materials. After the heat-treatment at 270 °C the specific surface area increases to 600 $\mathrm{m}^2\ \mathrm{g}^{-1}$ (Table 2) as the material becomes more particulate and rougher.

Oxidation reactions: in order to check the catalytic activity of the prepared MeP**NHG** materials, a diagnostic substrate, (*Z*)-cyclooctene, was subjected to oxidation at room temperature and pressure. (*Z*)-Cyclooctene is a reactive alkene that has been used in previous studies with both homogeneous and heterogeneous catalysts, and as a product of the oxidation reaction we observe the formation of only cyclooctene oxide.[10,25a] The catalysis results are shown in Table 2. For comparison of the catalytic activity of MeP**NHG** materials with the same metalloporphyrin in homogeneous solution, all reaction conditions were maintained constant.

Controls for all reactions were carried out in the absence of catalyst (MeP**NHG** or homogeneous MeP) and in the presence

Table 2 Porphyrin loading, surface area and catalytic activity of MeP**NHG** in the oxidation of (*Z*)-cyclooctene using PhIO or H_2O_2 as oxygen donor

				Cyclooctene epoxide yield (% ± 5)	
Catalyst	Oxygen donor	MeP loading/mg g^{-1}	Surface area/$\mathrm{m}^2\ \mathrm{g}^{-1} \pm 10$	1 h	24 h
—	PhIO	—	—	0	0
NHG	PhIO	0	—	2	20
FeTFPPCl[10]	PhIO	—	—	89	89
FeP**NHG** (60 °C)	PhIO	18	5	10	100
FeP**NHG** (270 °C)	PhIO	18	600	33	45
FeTFPP–IPG[10]	PhIO	4	—	50	85
FePS–py[7b]	PhIO	3	142	43	85
MnTFPPCl[7b]	PhIO	—	—	84	84
MnP**NHG** (60 °C)	PhIO	18	5	10	75
MnP**NHG** (270 °C)	PhIO	18	600	27	55
MnPS–py[7b]	PhIO	3	132	0	34
MnP**NHG** (60 °C)	H_2O_2	18	5	0	13

Reaction conditions: $T = 25$ °C, magnetic stirring, solvent = 1,2-dichloroethane, (*Z*)-cyclooctene : oxygen donor : FeP molar ratio $1.2 \times 10^4 : 100 : 1$, [FeP] in both homogeneous and heterogeneous reaction $= 3.0 \times 10^{-4}\ \mathrm{mol\ L}^{-1}$, [oxygen donor] $= 5.7 \times 10^{-3}\ \mathrm{mol\ L}^{-1}$.

of alumina **NHG** without MeP. The control reactions showed that in the absence of MeP and alumina no detectable oxidation of substrate occurred. We observed that alumina without MeP (**NHG**) can catalyse cyclooctene oxidation using PhIO as oxygen donor in yields of up to 20% after 24 h. Acosta *et al.*[13] detected the presence of Al^V sites in alumina prepared by the non-hydrolytic process in gels dried at up to 150 °C, suggesting a special catalytic activity related to them. We argue that the cyclooctene epoxide yields in the **NHG** are due to the presence of these Al^V sites in the material.

In all of the reactions PhIO was totally consumed and the PhI yields were *ca.* 100%, showing that all of the oxidant was converted to PhI and that the competitive reaction between the active intermediate and another molecule of PhIO, forming $PhIO_2$, does not occur.[25b]

MeP**NHG** heat-treated at 60 °C led to cyclooctene epoxide yields comparable to those obtained with the corresponding MeP in homogeneous solution (Table 2). Slightly better product yields are obtained with FeP**NHG** than with homogeneous FeP, since the entrapment of FeP prevents the formation of dimeric species.

We observe in Table 2 that after 1 h of reaction, the MeP**NHG** heat-treated at 270 °C shows higher epoxide yield than that heat-treated at 60 °C, implying higher initial epoxidation ratio in the materials heat-treated at 270 °C, and we argue that this is due to the higher surface area of these materials (600 $m^2 g^{-1}$). This behaviour can be explained by the changing of the pore structures during the heat treatment.[26] It is likely that the active catalytic site in the materials treated at higher temperature is more accessible than in the materials treated at 60 °C, favouring the approach of the substrate (*Z*)-cyclooctene and the diffusion of the product *cis*-epoxycyclooctane from the heterogeneous catalyst into the bulk solution.[25,27] However, after 24 h of reaction, despite the higher surface area of MeP**NHG** heat-treated at 270 °C (600 $m^2 g^{-1}$, *cf.* 5 $m^2 g^{-1}$), the materials heat-treated at 60 °C are better catalysts (cyclooctene oxide yields 100 and 75% for FeP**NHG** and MnP**NHG**, respectively). When longer reaction times are used, the increase in surface area of the MeP**NHG** catalyst is in the opposite direction to the decrease in its activity. We attribute this result to the higher porosity and fragility of the alumina matrix after its heat-treatment at 270 °C. After 1 h of stirring these porous materials can be easily broken into more compact materials. In this process part of the pores can be blocked and access of the substrate to the FeP site is inhibited. The MeP**NHG** samples heat-treated at 60 °C are more compact and are less fragile than the former catalyst. Although the MeP**NHG** materials heat-treated at 60 °C have smaller initial epoxidation ratios (due to the presence of a smaller number of pores in the matrix), they are not broken during the stirring process and are consequently active for a longer period than the MeP**NHG** materials heat-treated at 270 °C, presenting higher product yields at the end of the reaction. Further studies are being carried out by our group to prove this.

When MeP**NHG** were used as catalysts, the UV–Vis spectra of the reaction solutions showed no evidence for any leached FeP or MnP and they were catalytically inactive when fresh PhIO was added to them.

The rate of (*Z*)-cyclooctene epoxidation with homogeneous MeP is faster than that with MeP**NHG** systems (Table 2). It has been observed that the epoxidation of (*Z*)-cyclooctene is ten times faster in FeP homogeneous systems than in a modified silica-supported system.[10,25,27] This difference in the rate of reactions can be assigned to the greater polarity of the matrix, which impedes the approach of a substrate to the catalytic active site and may slow down the diffusion of the product epoxide into the reaction medium.

The catalytic activities of MeP**NHG** were compared with those of supported MeP on imidazole propyl gel through a coordination bond (FeP–IPG)[10] and of hybrid organic–inorganic materials containing MeP covalently bonded to silica prepared by a sol–gel process (FePS and MnPS,[7] Table 2).

Table 3 MeP**NHG** recycling in the oxidation of (*Z*)-cyclooctene using PhIO as oxygen donor

Catalyst	Reaction	Cyclooctene epoxide yield (% ± 5) 1 h	24 h
NHG	First reaction	2	20
NHG	Recycling	4	20
FeP**NHG**	First reaction	10	100
FeP**NHG**	Recycling	1	48
MnP**NHG**	First reaction	10	75
MnP**NHG**	Recycling	1	35

Reaction conditions: $T = 25\,°C$, magnetic stirring, solvent = DCE, (*Z*)-cyclooctene : oxygen donor : FeP molar ratio = $1.2 \times 10^4 : 100 : 1$, $[FeP] = 3.0 \times 10^{-4}$ mol L^{-1}, $[PhIO] = 5.7 \times 10^{-3}$ mol L^{-1}.

MeP**NHG** and MeP–IPG materials show similar catalytic yields (Table 2). The advantage of MeP**NHG** materials is that MeP cannot be leached from the matrix, whereas the MeP coordinated to the IPG support can be extracted with more polar solvents such as methanol.[27]

The MnP**NHG** system is more active than the MnPS, whereas the FeP**NHG** present similar catalytic activity to FePS (Table 2). It has already been reported during MePS preparation *via* the sol–gel process, in the presence of a nitrogen base catalyst, $Me^{III}P$ reduction to $Me^{II}P$ can occur, leading to materials with low catalytic activity.[7b] In the MeP**NHG** materials we did not observe the reduction of $Me^{III}P$ to $Me^{II}P$, allowing better catalytic yields for the MeP**NHG** materials compared with those of MePS.

Recycling of the MeP**NHG** catalyst materials shows that their catalytic activity in the second reaction is half of that of the yield in the first reaction (Table 3). We observed that after the first reaction the MeP**NHG** materials were reduced to a finer powder when compared with the initial material. In fact, these porous solids that are used in catalysis are often in the form of powders whose surface obeys fractal scaling laws and appears to have $D = 3$. Their tenuous structure renders them weak when subjected to the mechanical stress of grinding, breaking them into more compact particles which are relatively smooth.[28] Apparently, the stirring procedure utilised during the oxidation reaction fragmented the support, leading to the formation of fines in the reaction medium. These fines can be responsible for clogging of the pores of the support, leading to the lower catalytic yields in the second reaction. Although we observed this decrease in the catalytic activity in the recycling reaction, the solid catalysts do have the advantage of being easily recovered at the end of the reaction.

Very low yields were observed for cyclooctene oxidation when H_2O_2 is used as oxygen donor using MnP**NHG** as catalyst (13% yield, Table 2). The desired hydrogen peroxide activation route in the case of synthetic MeP is the heterolytic mode that leads to the generation of a water molecule and a high-valent metal–oxo porphyrin complex. Fast side-reactions between the intermediates and another H_2O_2 results in low product yields.[29,30] These side-reactions are probably favoured by the presence of the alumina support in the environs of the intermediate.

4 Conclusion

Novel hybrid organic–inorganic catalysts constituted of iron(III) and manganese(III) 5,10,15,20-tetrakis(pentafluorophenyl) porphyrin entrapped in an alumina gel matrix have been prepared by a non-hydrolytic route through the condensation of aluminium chloride with diisopropyl ether in the presence of

MeP. Using this procedure, 100% of MeP remained entrapped and leaching was not observed even in the presence of polar solvents such as methanol. The alumina obtained after drying was amorphous and non-hydrated. The use of a conventional hydrolytic sol–gel process leads to complete leaching of the metalloporphyrin from the matrix, underlining the importance of the non-hydrolytic alumina gel process in the matrix preparation.

The new catalysts prepared were tested for their ability to catalyse the epoxidation of (*Z*)-cyclooctene using iodosylbenzene as oxygen donor, giving high yields in the epoxidation, similar to those obtained using the MeP in solution or supported on a silica matrix (IPG or MePS). The advantage of MeP**NHG** is that the MeP cannot be leached from the matrix during the epoxidation reaction.

Acknowledgements

We thank J. B. Valim for TGA/DTA analyses. Financial support from FAPESP, and CNPq are gratefully acknowledged.

References

1 R. A. Sheldon, in *Metalloporphyrins in Catalytic Oxidations*, ed. R. A. Sheldon, Marcel Dekker Inc., New York, 1994, ch. 1, p. 1.

2 B. Meunier, *Chem. Rev.*, 1992, **92**, 1411.

3 D. Mansuy, *Coord. Chem. Rev.*, 1993, **125**, 129.

4 J. R. Lindsay-Smith, in *Metalloporphyrins in Catalytic Oxidations*, ed. R. A. Sheldon, Marcel Dekker Inc., New York, 1994, ch. 11, p. 325.

5 A. Choplin and F. Quignard, *Coord. Chem. Rev.*, 1998, **178**, 1679.

6 P. Battioni, E. Cardin, M. Louloudi, G. Schollhorn, G. A. Spyroullias, D. Mansuy and T. G. Traylor, *Chem. Commun.*, 1996, 2037.

7 (*a*) K. J. Ciuffi, H. C. Sacco, J. B. Valim, C. M. C. P. Manso, O. A. Serra, O. R. Nascimento, E. A. Vidoto and Y. Iamamoto, *J. Non-Cryst. Solids*, 1999, **247**, 146; (*b*) K. J. Ciuffi, H. C. Sacco, J. C. Biazzotto, O. A. Serra, O. R. Nascimento, E. A. Vidoto, C. A. P. Leite and Y. Iamamoto, *J. Non-Cryst. Solids*, 2000, **273**, 108; (*c*) H. C. Sacco, J. C. Biazzotto, K. J. Ciuffi, O. A. Serra, O. R. Nascimento, M. R. Zuchi, C. A. P. Leite and Y. Iamamoto, *J. Non-Cryst. Solids*, 2000, **273**, 150; (*d*) Y. Iamamoto, H. C. Sacco, J. C. Biazzotto and K. J. Ciuffi, *An. Acad. Bras. Cienc.*, 2000, **72**, 59.

8 J. Quartararo, J.-P. Amoureux and J. Grimblot, *J. Mol. Catal., A: Chem.*, 2000, **162**, 353.

9 R. E. Kirk and D. F. Othmer, in *Encyclopedia of Chemical Technology*, ed. M. Howe-Grant, Wiley-Interscience, New York, 1991, vol. 2, pp. 291–330.

10 C. M. C. Prado-Manso, E. A. Vidoto, F. S. Vinhado, H. C. Sacco, K. J. Ciuffi, P. R. Martins, A. G. Ferreira, J. R. Lindsay-Smith, O. R. Nascimento and Yassuko Iamamoto, *J. Mol. Catal., A: Chem.*, 1999, **150**, 251.

11 J. S. Lindsey, I. C. Schreiman, H. C. Hsu, P. C. Kearney and A. M. Marguerettaz, *J. Org. Chem.*, 1987, **52**, 827.

12 A. D. Adler, F. R. Longo, F. Kampas and J. Kim, *J. Inorg. Nucl. Chem.*, 1970, **32**, 2443.

13 S. Acosta, R. J. P. Corriu, D. Leclerq, P. Lefèrvre, P. H. Mutin and A. Vioux, *J. Non-Cryst. Solids*, 1994, **170**, 234.

14 M. Dalibart and J. Deroualt, *Coord. Chem. Rev.*, 1986, **74**, 1.

15 Y. Kurokawa, T. Ishizaka, T. Ikoma and S. Tero-Kubota, *Chem. Phys. Lett.*, 1998, **287**, 737.

16 S. Brunauer, P. H. Emmett and E. Teller, *J. Am. Chem. Soc.*, 1938, **60**, 309.

17 A. H. Cardoso, C. A. P. Leite and F. Galembeck, *Langmuir*, 1998, **14**, 3189; L. Reimer, U. Zepke, J. Moesch, St. Schulze-Hillert, M. Messemer, W. Probst and E. Weimer, in *EELS Spectroscopy: A Reference Handbook of Standard Data for Identification and Interpretation of Electron Energy Loss Spectra and for Generation of Electron Spectroscopic Images*, ed. C. Zeiss, Oberkochen, Germany, 1992.

18 (*a*) J. G. Sharefkin and H. Saltzmann, *Org. Synth.*, 1963, **43**, 62; (*b*) H. J. Lucas, E. R. Kennedy and M. W. Forno, *Org. Synth.*, 1963, 483.

19 R. J. P. Corriu, D. Leclerq, P. Lefèrvre, P. H. Mutin and A. Vioux, *J. Mater. Chem.*, 1992, **2**, 673; R. J. P. Corriu and D. Leclerq, *Angew. Chem., Int. Ed. Engl.*, 1996, **35**, 1420.

20 F. Bèlanger-Garièpy, K. Hoogsteen, V. Sharma and J. D. Wuest, *Inorg. Chem.*, 1991, **30**, 4140.

21 T. P. Wijesekera and D. Dolphin, in *Metalloporphyrins in Catalytic Oxidations*, ed. R. A. Sheldon, Marcel Dekker Inc., New York, 1994, ch. 7, p. 193.

22 K. Ozette, P. Battioni, P. Leduc, J. F. Bartoli and D. Mansuy, *Inorg. Chem. Acta*, 1998, 272.

23 A. Gold, K. Jayaraj, P. Doppet, R. Weiss, G. Choltard and E. Bell, *J. Am. Chem. Soc.*, 1988, **110**, 177.

24 A. J. Léonard, F. Van Cauwelaert and J. J. Fripiat, *J. Phys. Chem.*, 1967, **71**, 695.

25 (*a*) P. R. Cooke and J. R. Lindsay-Smith, *J. Chem. Soc., Perkin Trans. 1*, 1994, 1913; (*b*) J. Nappa M and C. A. Tolman, *Inorg. Chem.*, 1985, **24**, 4711.

26 E. Seker, J. Cavataio, E. Gulari, P. Lorpongpaiboon and S. Osuwan, *Appl. Catal., A*, 1999, **183**, 121.

27 C. Gilmartin and J. R. Lindsay-Smith, *J. Chem. Soc., Perkin Trans. 2*, 1995, 243.

28 A. Harrison, in *Fractals in Chemistry*, Oxford Chemistry Primers, Oxford University Press, New York, 1995.

29 W. Nam, H. J. Lee, S. Y. Oh, C. Kim and H. G. Jang, *J. Inorg. Biochem.*, 2000, **80**, 219; Y. M. Goh and W. Nam, *Inorg. Chem.*, 1999, **38**, 914.

30 T. G. Traylor, C. Kim, W. P. Fann and C. L. Perrin, *Tetrahedron*, 1998, **54**, 7977.